

MAGNETIC AND PHYSICAL-MECHANICAL PROPERTIES OF WOOD PARTICLEBOARDS COMPOSITE FABRICATED WITH Fe_3O_4 NANOPARTICLES AND THREE PLANTATION WOODS

R. Moya^{*†}

Professor

E-mail: rmoya@itcr.ac.cr

J. Gaitán-Alvarez

Research Scientist

E-mail: jgaitan@itcr.ac.cr

A. Berrocal

Professor

Escuela de Ingeniería Forestal

Instituto Tecnológico de Costa Rica

Apartado 159-7050, Cartago, Costa Rica

E-mail: aberrocal@itcr.ac.cr

K. J. Merazzo

Researcher

BCMaterials, Basque Center for Materials, Applications and Nanostructures

UPV/EHU Science Park

48940 Leioa, Spain

Escuela de Física

Universidad de Costa Rica

San Pedro 11501-2060, Costa Rica

Materials Science and Engineering Research Center (CICIMA)

Universidad de Costa Rica

San Pedro, Costa Rica

and

Instituto Tecnológico de Costa Rica

Escuela de Física

Apartado 159-7050, Cartago, Costa Rica

E-mail: karlamerazzo@gmail.com

(Received February 2023)

Abstract. This study has the main objective to synthesize in situ Fe_3O_4 nanoparticles (NPs) in fiber particles of three tropical wood (*Pinus oocarpa*, *Vochysia guatemalensis*, and *Vochysia ferruginea*) using two different solutions of Fe^{3+} and Fe^{2+} in an aqueous ammonia solution. The magnetic properties were measured by determining fiber particles' Fe_3O_4 magnetization parameters (coercivity, remanence, and saturation magnetization). The Fourier transform IR and X-ray diffraction spectra were also obtained. After the magnetic wood particleboard (MWPC) was fabricated with 100% magnetic particles (MWPC-100) and a superficial layer magnetized with fiber (MWPC-layer), their physical, mechanics, and magnetic properties were compared. The results showed that Fe_3O_4 NPs content was similar in two Vochyseas species but higher than *Pinus oocarpa*. Ash content was similar in the three species. It was difficult to demonstrate the presence of Fe_3O_4 NPs in the FT-IR spectrum. The diameter of NPs varied from 51 to 68 nm and the saturation magnetization parameters were low, but these values were higher in *Pinus oocarpa*. MWPC showed that the use of NPs decreases the density of *Pinus oocarpa* but increases the density of the Vochyseas

* Corresponding author

† SWST member

species. Swelling and moisture absorption increased in the MWPC-100 of *Pinus oocarpa* and *Vochysia guatemalensis* but decreased in *Vochysia guatemalensis* composite. The internal bond decreased in MWPC-100, but not in the MWPC layer. Hardness increased in the MWPC layer in *Pinus oocarpa*, but not in MWPC-100, and this property increased in MWPC-100 and the MWPC layer fabricated with *Vochysia ferruginea* and *Vochysia guatemalensis*.

Keywords: Wood composites, wood-based magnetic composites, magnetic properties, tropical wood, wood modification, applied magnetics.

INTRODUCTION

The increasing use of electronic and wireless devices in people's daily lives, such as mobile phones, wireless networks, and home robots, are increasingly generating electromagnetic waves, affecting health in an unprecedented way (Oka et al 2012; Lou et al 2018a). Due to this situation, there is a need to reduce the source of unwanted radiation or reduce its impact on the surrounding area (Oka et al 2012). Several recent works of research have been carried out on the development of materials that are lightweight, which have low thicknesses with the ability to reduce or block electromagnetic waves (Lou et al 2018b; Lv et al 2018).

The combination of magnetic materials with lightweight dielectric materials has been studied, taking advantage of the synergistic effect between the two components (Liu et al 2012; Zheng et al 2014). Among these materials, modified wood has been studied as a material that blocks magnetic waves, which is a renewable and naturally degradable material, highly attractive as a biologically based composite material (Oka et al 2007, 2009; Rahayu et al 2022). The Oka group (Oka et al 2002), more than two decades ago, experimented with wood as a material that blocks electromagnetic waves by proposing the impregnation of magnetic powder inside the wood (Oka et al 2002, 2004a).

Nowadays, three different methods of fabrication of magnetic wood composites have been studied: impregnation of nanoparticles (NPs) of iron in combination with different solvents (Oka et al 2009), powder-type made of magnetic and wood materials, mixed with resins and then pressed under temperature (Oka et al 2007) and wood coatings with magnetic substances (Oka et al 2004b). Among the different methods studied, the impregnation of pretreated wood in a mixed

solution with ferrite NPs as Fe_3O_4 (Gan et al 2016), CoFe_2O_4 (Gan et al 2017a), and MnFe_2O_4 (Wang et al 2017) are the methods that stand out. This synthesis of the magnetic material within the wood occurs by in situ coprecipitation of the ferrite NPs through a chemical reaction of two sources of Fe^{3+} and Fe^{2+} in an aqueous solution, followed by impregnation with an ammonia solution, all this under a vacuum-pressure process (Dong et al 2016; Lou et al 2018a; Mashkour and Ranjbar 2018).

However, wood can come in different forms, from solid wood, through veneers, to particles, and each form will have a different performance/efficiency in the impregnation of Fe^{3+} and Fe^{2+} sources in solution. For shielding or deviating direct magnetic fields, the magnetic susceptibility is the magnetic property that defines the efficiency of the material, and it can be calculated or obtained by the hysteresis loop. When recounting the different ways in which wood has been investigated, the wood solid shape has had the greatest interest and has been investigated in different species, such as *Scots pine* (Garskaite et al 2021), *Populus tormentosa* (Dong et al 2015), fir woods (Gao et al 2012), *Picea abies*, *Fagus sylvatica* (Oka et al 2004a; Dong et al 2015), and poplar wood (Gan et al 2017a). In wood shavings, poplar wood (Mashkour and Ranjbar 2018) and *Populus deltoides* (Mashkour and Ranjbar 2018) have been investigated. Sawdust was magnetized in fir wood and cedar wood (Oka et al 2004a; Lou et al 2019b) and wood in the shade of flours or veneer was tested in two species of *Populus* (Mashkour and Ranjbar 2018; Lou et al 2019b). The wood fiber shape, flour or veneer, was poorly investigated, although *Populus* spp. and cedar wood reported magnetic properties (Trey et al 2014; Dong et al 2015).

The shape of the wood will determine the degree of penetration of the solution in the liquid state (Bolton and Humphrey 1994). Therefore, a solution from a ferrous source, for the in situ formation of NPs, will also depend on the shape of the wood. For example, in the case of solid wood the penetration depends on the permeability of the wood, in the case of veneer the permeability is less important, since, in general, the thicknesses are not greater than 3 mm; and in the case of shaped wood particle, the thickness is small and the dimensions are big enough to have a greater contact surface between the wood and the iron solutions (Bolton and Humphrey 1994). Thus, it is necessary to investigate different forms of wood for different species.

Another important aspect of the technique of magnetizing the wood in situ, in addition to the shape of the wood, is the species; this method has been applied to different species, such as the genus *Populus*, *Picea abies*, poplar and fir woods, *Scots pine*, *Fagus sylvatica*, and cedar sapwood (Oka et al 2004a; Gao et al 2012; Dong et al 2015; Gan et al 2017a; Mashkour and Ranjbar 2018; Lou et al 2019b; Garskaite et al 2021). These studies have been limited to species of temperate climate.

Recently, Moya et al (2022) carried out the first investigations in tropical woods, applying the in-situ method with good results of coercivity (Hc), retentivity (Mr), and saturation magnetization (Ms) in two different species. They concluded that the use of the method of in situ synthesis of the magnetic material within the wood is appropriate. However, the amount of NPs added is not adequate to achieve high values of Hc, Mr, and Ms. Several authors point out the weaknesses of this method, which can be applied to the results obtained in tropical woods. Lou et al (2019b) and Trey et al (2014) pointed out that the dipolar forces between the impregnated particles easily add to each other forming conglomerates, affecting the uniformity of the particle deposition in different parts of the magnetic wood. Also, Lou et al (2019b) and Trey et al (2014) argued that indeed the magnetic particles mixed with polymers and wood in large quantities lead to brittle compounds, a situation that restricts

the adequate application of the particles in the wood in situ.

Other studies (Oka et al 2007; Lou et al 2018b) have described the in situ method as the one that uses immersion impregnation of solid wood or veneer although without the vacuum pressure. Therefore, the impregnation is superficial. Oka et al (2007) noted that low values of Hc, Mr, and Ms in solid wood or veneer are due to the superficial impregnation as it is not possible to control the shape and size of the surface. The process is not feasible and the magnetic particles cannot be deposited properly. Another cause of low values of magnetization parameters is that the surface of the wood is rich in hydroxyl groups, which are electronegative in aqueous solutions, so they are not attractive for assembling layers of NPs on the surface (Tang and Fu 2020). Rao et al (2016) and Rennekar and Zhou (2009), demonstrated that impregnation of wood superficially through the union of polyelectrolytes. However, despite these important advances, the manufacture of magnetic fiber boards by chemical surface coprecipitation, together with the investigation of the properties of magnetic field-blocking of the wood, is limited (Bolton and Humphrey 1994; Dong et al 2015; Lou et al 2018a).

Magnetizing the particles of wood has the advantage of, as we have indicated, a greater contact area (Bolton and Humphrey 1994). Therefore this would be one more option to increase the magnetic properties of tropical woods.

On the other hand, reforestation programs for wood production have been implemented with fast-growing hardwoods using a wide variety of species (Tenorio et al 2016). Recently different methods to improve wood properties such as dimensional stability, MC, biodeterioration, and durability, have been investigated, among which mineralization, acetylation, furfurylation, and densification modification have been achieved (Gaitán-Alvarez et al 2020a, 2021; Moya et al 2020). In addition, in situ magnetized wood has been previously studied in tropical woods with good results in Hc, Mr, and Ms values. However, the amount of NPs added is not adequate to achieve higher

values of these magnetic values (Moya et al 2022).

Therefore, to produce tropical wood species with adequate magnetic properties, this work elaborates magnetic wood particleboards composite (MWPC) with NPs synthesized in situ with $\text{FeCl}_3 \cdot 6\text{H}_2\text{O}$, $\text{FeCl}_2 \cdot 4\text{H}_2\text{O}$, as a source of Fe^{3+} and Fe^{2+} , using the wood of three different tropical species from fast-growth plantations in Costa Rica: *Pinus oocarpa*, *Vochysia ferruginea*, and *Vochysia guatemalensis*. The characterization consists of obtaining the physical properties (density, thickness, swelling, and water absorption), mechanical properties (internal bond and hardness), chemical properties (Fourier transform IR [FTIR] and X-ray diffraction [XRD]), and magnetic properties (vibrating sample magnetometry [VSM]) of wood fiber particles and wood boards.

MATERIALS AND METHODS

Experimental Materials

The reagents used were iron (III) hexahydrate ($\text{FeCl}_3 \cdot 6\text{H}_2\text{O}$) $\geq 98\%$; iron (II) chloride tetrahydrate ($\text{FeCl}_2 \cdot 4\text{H}_2\text{O}$) $\geq 98\%$; ammonium hydroxide solution at 30%; and absolute ethyl alcohol and toluene.

Sapwood particles of *Pinus oocarpa*, *Vochysia ferruginea*, and *Vochysia guatemalensis* extracted from trees from fast-growing forest plantations in Costa Rica, which have shown good permeability of liquids (Gaitán-Alvarez et al 2020a), were used. These species have shown excellent absorption of different substances by different treatments that have been used to improve their wood properties, such as dimensional stability and resistance to biodeterioration and fire (Gaitán-Alvarez et al 2020a, 2020b; Moya et al 2020). Likewise, the solid wood of these three species has shown acceptable magnetic properties when they were copolymerized in situ with NPs of Fe_3O_4 using the two solutions of Fe^{3+} and Fe^{2+} .

Preparation Wood Particles

For the three species, all logs were first chipped and then milled in a Nogueira DPM-2 blade-hammer

mill using a sieve with 5 mm diameter holes. The particles were dried to an MC of approximately 8%. Then, the particles were screened and two sizes were selected to fabricate the composites: 1) particles between 4.9 and 3.0 mm were called large particles and 2) particles between 2.9 and 1.5 mm were called small particles.

In-situ Precipitation

The *in situ* precipitation of NPs Fe_3O_4 was carried out according to Dong et al's (2016) methods was carried out. Firstly, the wood particles were pretreated: 2 kg of each particle size were placed in 20 L (l) of distilled water and heated for 2 h (h), to extract the largest amount of water-soluble extractives. This process was repeated approximately 10 times until the water turned clear. The particles were then dried to constant MC in an oven at 105°C for 24 h. Then, the dried wood particles were placed with a solvent mixture of alcohol/toluene (1:2, V/V) overnight to remove the wood extractive compounds, such as gums, tropolones, fats and fatty acids, and to improve the surface affinity for the iron salts. After this time, the alcohol was allowed to evaporate and then the two groups of particles were dried at 4% MC in an oven. Next, a mixture solution of $\text{FeCl}_3 \cdot 6\text{H}_2\text{O}$ and $\text{FeCl}_2 \cdot 4\text{H}_2\text{O}$ (molar ratio of $\text{Fe}^{3+} : \text{Fe}^{2+} = 2:1$) was prepared and dissolved in distilled water to form the iron precursor solution with a concentration of 0.45 mol L⁻¹ ferric chloride. The pretreated wood particles were impregnated in the mixture for 12 h, at atmospheric pressure. The particles were filtrated and washed several times with distilled water to remove the residual iron salts on the surface. Then, the particles were dried at 65°C for 12 h and were again impregnated in a 25% ammonia solution for 12 h. Again, the wood particles were filtrated and washed several times with distilled water until reaching neutral pH, and then, the particles were dried at 65°C for 24 h to reach 4% of MC.

Characterization of the Wood Particles

The Fe_3O_4 NPs content formed and the ash content was determined for each species and each

treatment (untreated and treated). Three samples were taken with a size of 420 μm to 250 μm (40 and 60 mesh, respectively). The Fe_3O_4 NPs content was measured by direct aspiration in an atomic absorption spectrometer (AAnalyst 800, SpectraLab Scientific Inc, CA), following the ASTM D6357-19 standard (ASTM 2021). Then, the amount of Fe_3O_4 in the wood was calculated by Eq (1). The ash content was determined according to ASTM-D1102-84 (ASTM 2013).

$$\text{Fe}_3\text{O}_4 \left(\frac{\text{mg}}{\text{kg wood}} \right) = \frac{\text{Ash content}_{\text{sample}}(\%)}{100} \times \frac{\text{Fe}_3\text{O}_4 \text{ content}_{\text{sample}}(\text{mg})}{1_{\text{ash}}(\text{g})} \times \frac{1000_{\text{ash}}(\text{g})}{1_{\text{ash}}(\text{kg})}, \quad (1)$$

where Ash content sample: ash percentage obtained in the laboratory.

FTIR spectroscopy. For each species, three different samples were obtained, for both treated and untreated-sample particles, with a size of 420 μm to 250 μm (40 and 60 mesh, respectively) and dried at 0% of MC (MC). FTIR spectroscopy scanning was performed on the samples using a Nicolet 380 FTIR spectrometer (Thermo Scientific, Mundelein, IL) with a single reflecting cell (equipped with a diamond crystal). The equipment was configured to perform readings accumulating 32 scans with a resolution of 1 cm^{-1} , with a background correction before each measurement. The FTIR spectra obtained were processed with Spotlight 1.5.1, HyperView 3.2, and Spectrum 6.2.0 software developed by Perkin Elmer Inc. (Waltham, MA). The main vibrations where the greatest changes in the wood occurred were identified according to Dong et al (2016), Gao et al (2017), and Gan et al (2017a): the peak in 1251 cm^{-1} was related to C–O stretching vibration, the peak at 1505 cm^{-1} was attributed to the methylene and methyl groups in the saturated hydrocarbons, the peak at 1601 cm^{-1} to C=C aromatic skeletal vibrations of lignin components, the peak at 1739 cm^{-1} was assigned to the C=O

stretching in nonconjugated ketones and ester groups, the peak at 2901 cm^{-1} corresponded to $-\text{CH}_3$ asymmetric and the peak at 3340 cm^{-1} the absorption band assigned to the O–H stretching vibration of hydroxyl groups.

X-ray diffraction. The XRD spectrum was performed on the treated and untreated particles of the three species. The XRD spectrum was obtained on a PANalytical Empyrean Series 2 diffractometer (Malvern Panalytical Ltd, Malvern, United Kingdom) (Cu-K α , $6^\circ - 40^\circ 2\theta$), in conjunction with the PANalytical High Score Plus software. The particles were placed in a neoprene rectangle that was placed on a glass plate for measurement. The apparatus parameters were set as follows: Cu-K α radiation with a graphite monochromator, voltage 40 kV, electric current 40 mA, and 2 h scan range from 5° to 90° with a scanning speed of 2° min^{-1} . The average diameter of crystalline Fe_3O_4 NPs (D) in magnetic wood was evaluated based on its XRD pattern using the Scherrer Eq (2) (Lin and Ho 2014).

$$D = \frac{K\lambda}{(\beta \cos\theta)}, \quad (2)$$

where K is the X-ray wavelength (0.15418 nm), λ is the Scherrer constant (0.89), β is the peak full width at half maximum (FWHM), and θ is the Bragg diffraction angle.

Vibrating sample magnetometry. Three samples of the treated and untreated particles of the studied species were used. Three hundred microgram of particles were pelleted to a cylindrical shape of 5 mm diameter and 5 mm length. Then, the magnetic hysteresis loops (magnetization vs applied magnetic field) were determined at room temperature using a MicroSense EZ7 VSM, in an external magnetic field from -20 to 20 kOe in 2 Oe and 10 Oe steps at a low magnetic field, and in 100 and 500 Oe steps at higher fields, and an average time of 100 ms (Fig 1[a]). The M_s , H_c , and remanence (M_r) were extracted from the hysteresis loops. To evaluate the stability of the magnetic property in the acid environment, acid resistance tests were conducted by immersing the specimens

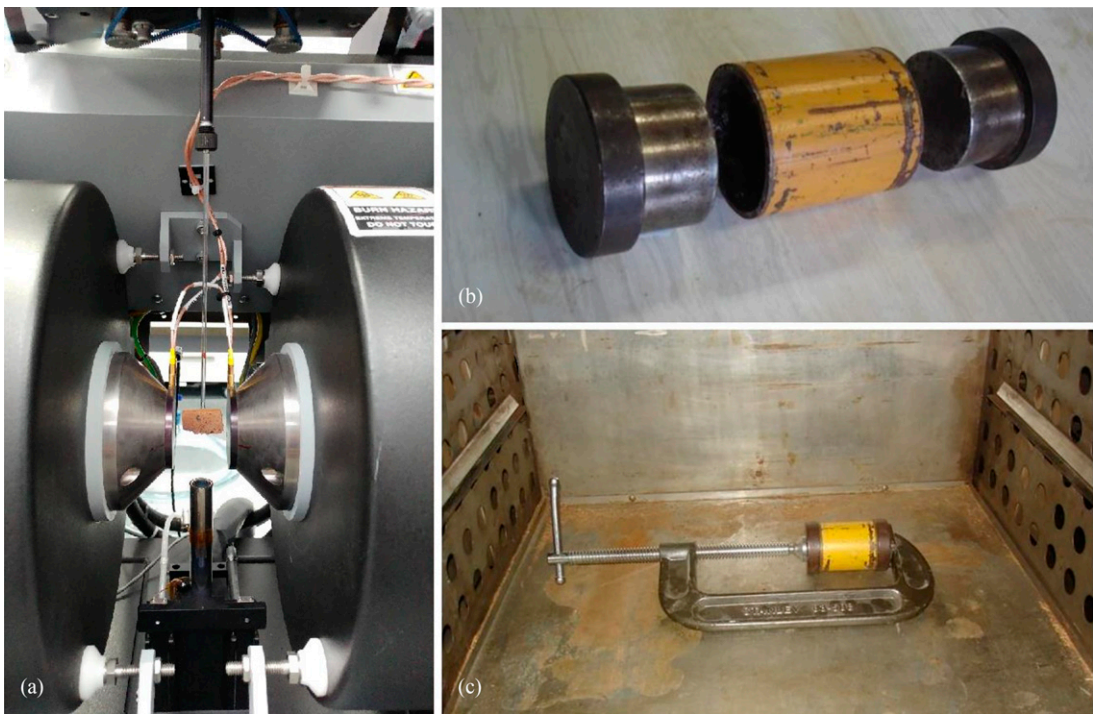


Figure 1. Vibrating sample magnetometer and location of composite sample (a), metal rack utilized (b), and press application during heating in the particleboards fabrication (c).

in 4% hydrochloric acid solution for 7 d. Then, the magnetic property was evaluated by VSM.

Preparation of MWPC

Three treatments of MWPC were fabricated with 12 mm thickness of the three species: 1) particleboards with untreated wood particles, 2) particleboards with 100% magnetic wood particles (MWPC-100), and 3) particleboards with two layers, one layer of 10 mm thickness with particles untreated and an external layer of 2 mm thickness with magnetic wood particles or treated (MWPC-layer). For the construction of MWPC, a small metal rack was built to make the specimens (Fig 1[b]), according to the methodology used by Moya-Roque et al (2014): 21 specimens for treatment were fabricated, for a total of 63 specimens per species. The fabrication of specimens was circular, with dimensions of 53 mm in diameter and 12 mm in thickness. The rack consisted of a 5 cm diameter metal pipe, 7 cm long with a plug at

each end introduced at a 2.9 cm depth as blocks, leaving a 12 mm gap in the middle that corresponds to the thickness of the test specimen. The particleboards specimen was fabricated at a density of approximately 0.70 g cm^{-3} and was made up of 90% coarse chips (4.9 to 3.0 mm) and 10% thin chips (2.9 to 1.5 mm). The particles were uniformly mixed and glued with urea formaldehyde in 10% proportion (weight/weight). Once the mixture was made, the rack was carefully filled and pressed until they filled up the 12 mm gap in the middle with the help of a manual press (Fig 1[c]), after which the semipressed tubes were transferred to a heat press for hot pressing. Using a pressure of 35 MPa at a temperature of 120°C for 30 min. Lastly, the samples were left for a 24 h room-temperature-conditioning period.

Physical Properties

The following physical properties of MWPC specimens were determined: density, thickness swelling,

and water and moisture absorption. The density was measured in all the specimens made in the three species; this was obtained by measuring volume and weight (weight/volume). To determine the thickness swelling and moisture absorption, five MWPC specimens in each treatment were conditioned and weighed at 12% EMC, and then conditioned for 3-4 wk at 18% EMC. After conditioning, the samples were weighed and measured again. This procedure was based on the ASTM D4933-99 norm (ASTM 1999) but modified to the conditions in Costa Rica, where environmental moisture conditions are around 18%. The thickness swelling was calculated using Eq 3. Moisture absorption was determined through Eq 4 by obtaining the percentage weight gain from 12% to 18% of MC with respect to dry weight. The difference between both moisture measurements (12% and 18%) represented the sample moisture absorption (Eq 5).

Swelling(mm)

$$= (g) \frac{\text{measurement } 12\% \text{ (mm)} - \text{measurement } 18\% \text{ (mm)}}{\text{measurement } 12\% \text{ (mm)}} \times 100 \quad (3)$$

Moisture content_{MC}

$$= \frac{\text{Weight}_{MC}(g) - \text{Weight}_{\text{oven-dried}}(g)}{\text{Weight}_{\text{oven-dried}}(g)} \times 100 \quad (4)$$

Moisture absorption = Moisture content_{18%}
- Moisture content_{12%}

(5)

For water absorption, another five MWPC specimens for each species/treatment previously weighed were immersed in water for 24 h. After this period, the samples were again weighed, and weight gain or water absorption was determined following Eq 5, according to ASTM D4446-13 (ASTM 1985).

Mechanical Properties

Mechanical properties tested were Janka hardness and internal bond. Janka hardness was determined for eight MWPC specimens per treatment in each species, according to ASTM D143-14 (ASTM

1999). The internal bond test was performed in accordance with the ASTM D1037-12 (ASTM 1999) standard, using another eight specimens per treatment in each species. All mechanical tests were performed on a Tinius Olsen H10KT universal testing machine.

Statistical Analysis

First, the normality and homogeneity of the data and the elimination of strange data or “outliers” of the variables evaluated were checked. Then a descriptive analysis was made, determining the average, standard deviation, and coefficient of variation for each variable studied. Then, analysis of variance was applied to determine the differences in the three treatments, where this represents the independent variable of the model and the measured variables as the dependent variables. Tukey’s test was used to determine the statistical significance of the difference between the means of the variables.

RESULTS AND DISCUSSION

Fe₃O₄ and Ash Content

The Fe₃O₄ content of MWPC varied between 176.26 and 466.307 mg kg⁻¹. The composites fabricated with three species were statistically different from untreated wood. The two *Vochysias* species have similar Fe₃O₄ content (Fig 2[a]), but *Pinus oocarpa* has the statistically lowest values of the three species. Ash values varied between 0.26% and 2.76% for untreated wood and between 3.28% and 4.86% for MWPC, with statistical differences observed in all species between untreated and MWPC (Fig 2[b]).

The retention of Fe₃O₄ NPs, measured by Fe₃O₄ content in ash, was variable in the three different tropical species. This variability is attributed to the fact that the species present different permeability to the flow of liquids within the wood (Thomas 1976). Moya et al (2022) explained that the anatomical structures of the three species used are different and that the species *Vochysia guatemalensis* and *Vochysia ferruginea* have anatomical elements that are more appropriate for fluid

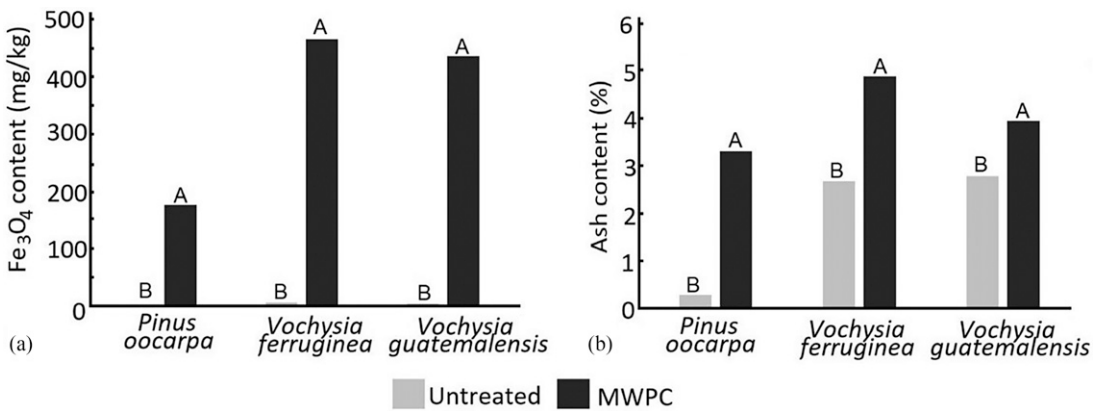


Figure 2. Fe₃O₄ (a) and Ash (b) content of magnetic wood particleboards composite (MWPC) of three tropical species from fast-growth plantations in Costa Rica. Note: Uppercase letters mean statistical differences between treatments at 95% significance.

flow. Thus, these two species achieve greater precipitation of the Fe₃O₄ NPs compared with *Pinus oocarpa* wood.

On the other hand, regarding the Fe₃O₄ content comparison of the three species with solid wood using the same in situ synthesis systems (Moya et al 2022), it was observed that the Fe₃O₄ content in *Pinus oocarpa* average was 817.19 mg kg⁻¹, it ranged from 1600 to 4298 mg kg⁻¹ in *Vochysia ferruginea* and the average is 1907 mg kg⁻¹ in *Vochysia guatemalensis* and the ash content values were from 3.5% to 4.11% for *Pinus oocarpa*, between 9.47% and 10.40% for *Vochysia ferruginea*, and between 6.51% and 7.85% for *Vochysia guatemalensis* in solid wood (Moya et al 2022). These value ranges of Fe₃O₄ and ash content in solid wood are higher than the values obtained when the wood was magnetized in fiber shape (Fig 2[b]). Therefore, although the formation of NPs was evident, it was lower than when it came to magnetizing solid wood.

The shape of the wood (solid or particle wood) will determine the degree of penetration of the solution in the liquid state (Bolton and Humphrey 1994). Therefore, a ferrous source solution, for the in situ formation of NPs, will also depend on the shape of the wood. In solid wood, the penetration depends on the permeability of the wood; in the case of wood in particle shape, the thickness

was small and there was a greater contact surface between the wood and the iron solutions (Bolton and Humphrey 1994). However, regardless of the shape of the wood to be magnetized, it is important to apply pressure during the process. In the case of the solid wood of these species, Moya et al (2022) concluded that the use of the method of synthesis of the magnetic material in situ within the wood was appropriate. However, in the case of the fiber shape, there was no application of pressure, so the ferrous solution was only superficial, and therefore, there was less formation of Fe₃O₄ NPs in relation to the solid wood, in which pressure was applied in the copolymerization process of the Fe₃O₄ content.

Chemical Composition: FTIR

Figure 3 shows only the FT-IR spectrum from 500 to 1800 cm⁻¹ (Fig 3[a-c]) and not the band from 1900 to 3500 cm⁻¹; this region represents the absorption bands assigned to the O-H stretching vibration of hydroxyl groups (3340 cm⁻¹) and the bands at 2901 correspond to -CH₃ asymmetric (Gan et al 2017b). The band from 500 to 1800 cm⁻¹ corresponds to the organic region of the wood and the presence of Fe₃O₄ formation (Garskaite et al 2021). In the case of the organic region, changes in the structure of cellulose, hemicellulose, and lignin are evident and to a different degree in each of the species (Fig 3). In the

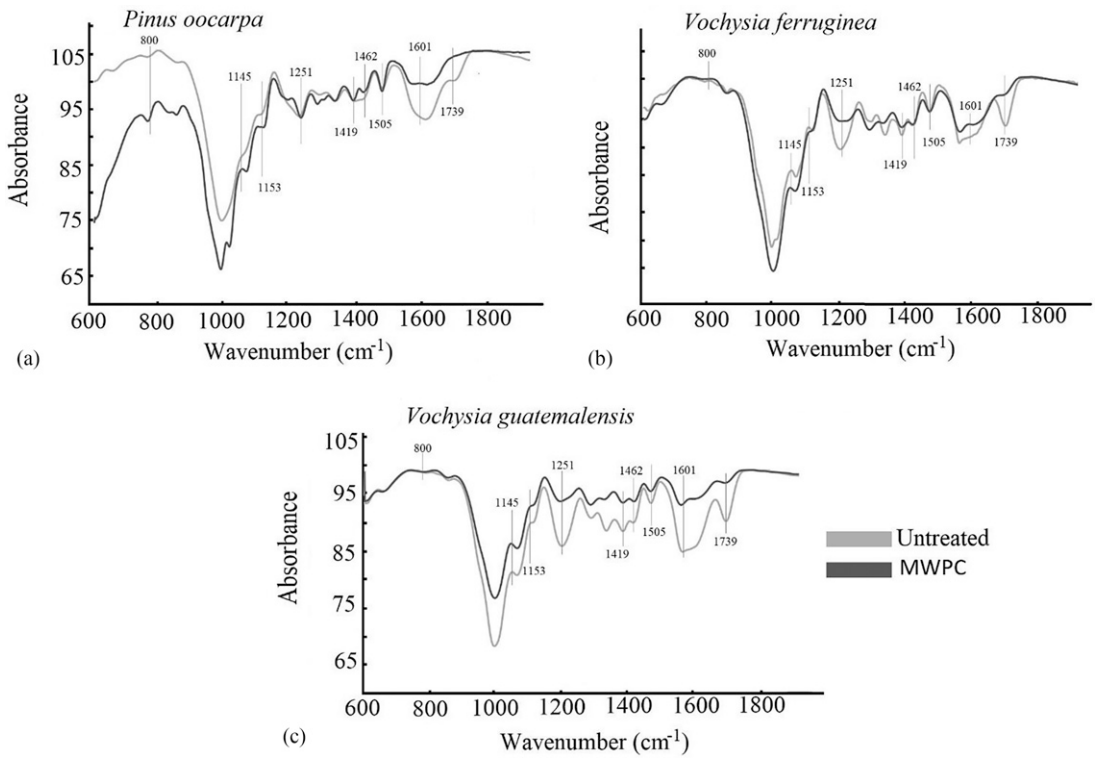


Figure 3. Fourier transform IR spectrum of magnetic wood particleboards composite (MWPC) of three tropical species (a-c) from fast-growth plantations in Costa Rica. a) *Pinus oocarpa* b) *Vochysia ferruginea* c) *Vochysia guatemalensis*. Note: Super-script letters mean statistical differences between treatments at 95% significance.

region of $500\text{--}800\text{ cm}^{-1}$, the presence of Fe_3O_4 in MWPC of different degrees in each of the species is also evidenced.

The wavelengths associated with the cellulose: 896 cm^{-1} show a heterophase carbon, and an increase in *Pinus oocarpa* (Fig 3[a]), but in both Vochyseas did not change (Fig 3[b] and [c]), the vibrations at 1054 cm^{-1} associated with C-H/C-O cellulose and 1090 associated with C-H/C-O cellulose (Lou et al 2018b) changed in the Vochyseas species (Fig 3[b] and [c]), but not in *Pinus oocarpa* (Fig 3[a]). While the vibration at 1145 cm^{-1} signal, stretching vibration of C-O in glucose of cellulose (Gao et al 2012), was similar in untreated and treated wood. Thus, the previous results indicate that there was a modification of cellulose in *Vochysia guatemalensis* and *Vochysia ferruginea* due to the magnetization, and *Pinus oocarpa* was less affected.

In the case of vibrations of the hemicellulose, the vibration at 1379 cm^{-1} is associated with C-H bending cellulose and hemicellulose (Yang et al 2020); these decreased only in the Vochyseas species, but not in *Pinus oocarpa*. The vibrations at 1601 and 1739 cm^{-1} , associated with the C=O stretching vibration absorption peak of hemicellulose (Yang et al 2020), decreased with the presence of magnetic particles in the three species and are associated with hemicellulose degradation (Gao et al 2012; Dong et al 2016; Gan et al 2017a, 2017b; Wang et al 2019; Garskaite et al 2021). Finally, the vibrations associated with lignin: 1601 cm^{-1} , which is associated with C=C aromatic skeletal vibrations (Garskaite et al 2021), and 1462 cm^{-1} , to an aromatic C=C stretching of aromatic rings of lignin, increased in the vochyseas (Fig 3[b] and [c]), but not in *Pinus oocarpa* (Fig 3[a]), 1505 cm^{-1} associated with lignin, did not show significant changes, peak at 1419 cm^{-1}

associated with C-H bonds of lignin, decreased in all three species and 1251 cm^{-1} associated with the ester linkage of carboxylic groups of the ferulic and p-coumaric acids of lignin (Lou et al 2019a) decreased in the vochyseas, but not in *Pinus oocarpa* (Fig 3[a]). Again, according to the results of the signals associated with hemicellulose and lignin, it is observed that the two species of Vochyseas (*Vochysia guatemalensis* and *Vochysia ferruginea*) showed greater degradation than *Pinus oocarpa*.

The formation of Fe_3O_4 in the wood samples is evident in the bands from minor to 800 cm^{-1} , specifically bands around 561 and 667 cm^{-1} . However, with the FTIR spectrum, it is difficult to demonstrate the formation of Fe_3O_4 , since they overlap with other signals, so, it is better to use techniques that measure the wavelength between

650 and 450 cm^{-1} (Lou et al 2019a, 2019b). Despite this drawback, a signal at 800 cm^{-1} obtained—corresponding to tetrahedral sites of the crystal lattice, which is due to the oxidation of Fe^{2+} and Fe^{3+} splits (Garskaite et al 2021)—increased mainly in the wood of *Vochysia ferruginea* and *Vochysia guatemalensis* (Fig 3[b] and [c]). In *Pinus oocarpa*, the peak is less evident (Fig 3[a]), thus confirming the low measurement of Fe_3O_4 content (Fig 2[a]) and the lesser formation in relation to the other two species of wood.

Crystalline Structure: XRD

The crystalline structures of untreated and treated specimens were characterized by XRD (Fig 4[a-c]). Untreated wood of the three species shows a typical diffraction angle at 20° due to cellulose (Cave and Walker 1994), which are 15.8° , 22.2° , and 34.6°

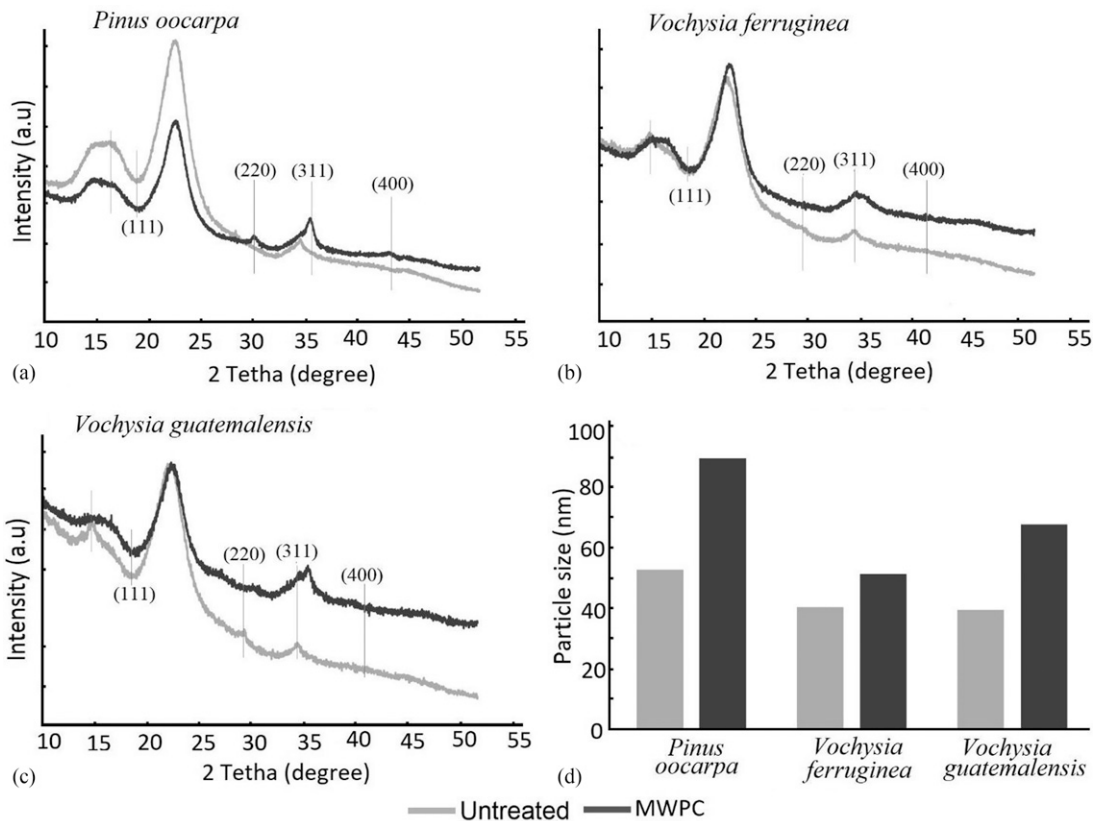


Figure 4. X-ray diffraction of magnetic wood particleboards composite (MWPC) (a-c) and particle size of Fe_3O_4 of three tropical species (d) from fast-growth plantations in Costa Rica.

corresponding to the planes (101), (102), and (400), respectively. But in samples with magnetized wood particles, two additional peaks are observed (at 15.8° and 22.2°), which belong to the cellulose and show that there were lightly weakened bonds of the cellulose. According to Dong et al (2016), these changes indicate that a part of the crystalline structure of the wood was damaged, confirming that the ammonia treatment affected the wood structure.

In addition, it was observed that diffraction angles at 20° , 30° , 35° , and 44° were more pronounced in the magnetic wood (Fig 4[a-c]). In the case of *Pinus oocarpa*, the peak was less intense at 30° and 35° representing (220) and (311), respectively (Fig 4[a]), which corresponds to the cubic phase with the space of $Fd\bar{3}m$ (Lou et al 2019a). In the magnetized *Vochysia ferruginea* and *Vochysia guatemalensis*, the peaks are placed at 35° (311) (Fig 4[b] and [c]). In the case of the *Pinus oocarpa*, the strongest diffraction peak is seen at 34° (311), in *Vochysia ferruginea*, the strongest peaks are at 30° and 35° and in *Vochysia guatemalensis*, the strongest peaks are at 30° , 35° , and 44° . These differences in patterns and particle size (determined using the Scherrer Eq 2) (Lin and Ho 2014) show that the amount of Fe_3O_4 NPs deposited was different in each of the species. The largest size was obtained in *Pinus oocarpa*, followed by *Vochysia guatemalensis* and the least size was obtained in *Vochysia ferruginea* (Fig 4[d]), which correspond to 89.58, 67.80, and 51.39, respectively. The particle sizes in *Pinus oocarpa* were in agreement with the values found by Mashkour and Ranjbar (2018). The values of *Vochyseas* species were slightly higher than those reported by Lou et al (2018b) and Gao et al (2012).

Magnetic Properties

Figure 5(a)-(c) shows the hysteresis curves of the untreated and magnetic wood particles. Representative magnetic properties, H_c , M_r , and M_s were extracted from these hysteresis curves, while the percentage of magnetic NPs present in the samples was calculated with the M_s of the magnetic NPs present in the samples; these values are presented

in Table 1. In the case of untreated wood, the hysteresis curves show negligible M_s (Fig 5), which is the expected behavior of wood (Kojima et al 2009).

On the other hand, the magnetized material, in all species, exhibited a clear hysteresis loop corresponding to ferromagnetic behavior (Fig 5), but large differences between species were found. For example, M_s was lowest in *Vochysia guatemalensis* (Fig 5[c]) and highest in *Pinus oocarpa* (Fig 5[a]), while *Vochysia ferruginea* had intermediate values (Fig 5[b]).

It has been observed that there is significant variation in the precipitation of Fe_3O_4 NPs between species, proving their different absorption capacity of NPs (Fig 2[a]). As indicated above, this variability is attributed to the permeability of the wood or the flow of fluids in it (Lin and Ho 2014), which varies depending on the anatomical elements present in the wood samples (Moya et al 2022).

An important aspect to highlight, regarding the values of H_c , M_r , and M_s of the species using fiber in this work, is that they presented lower values than when they are treated with solid wood (Moya et al 2022) or previous studies with other species (Dong et al 2016; Gan et al 2016). Although these latest studies have used other precipitation methods for Fe_3O_4 NPs, these low values may be associated with the low permeability of wood to the flow of liquid substances in the species studied (Gaitán-Alvarez et al 2020a, 2020b). However, an appropriate immersion time in ammonia had positive effects on the magnetic properties of wood (Lou et al 2018b; Moya et al 2022), which could increase the magnetic properties of wood when they are treated in the form of particles.

If we compare these values of M_s (Table 2) with the NP content of Fe_3O_4 (Fig 2[a]), the highest value of M_s in *Pinus oocarpa* (Table 2) contrasts with the lowest contents of Fe_3O_4 , while the M_s values of *Vochysia guatemalensis* and *Vochysia ferruginea* are low, but with high values of Fe_3O_4 content (Fig 2[a]). This inconsistent behavior across species could be because there are inhomogeneities

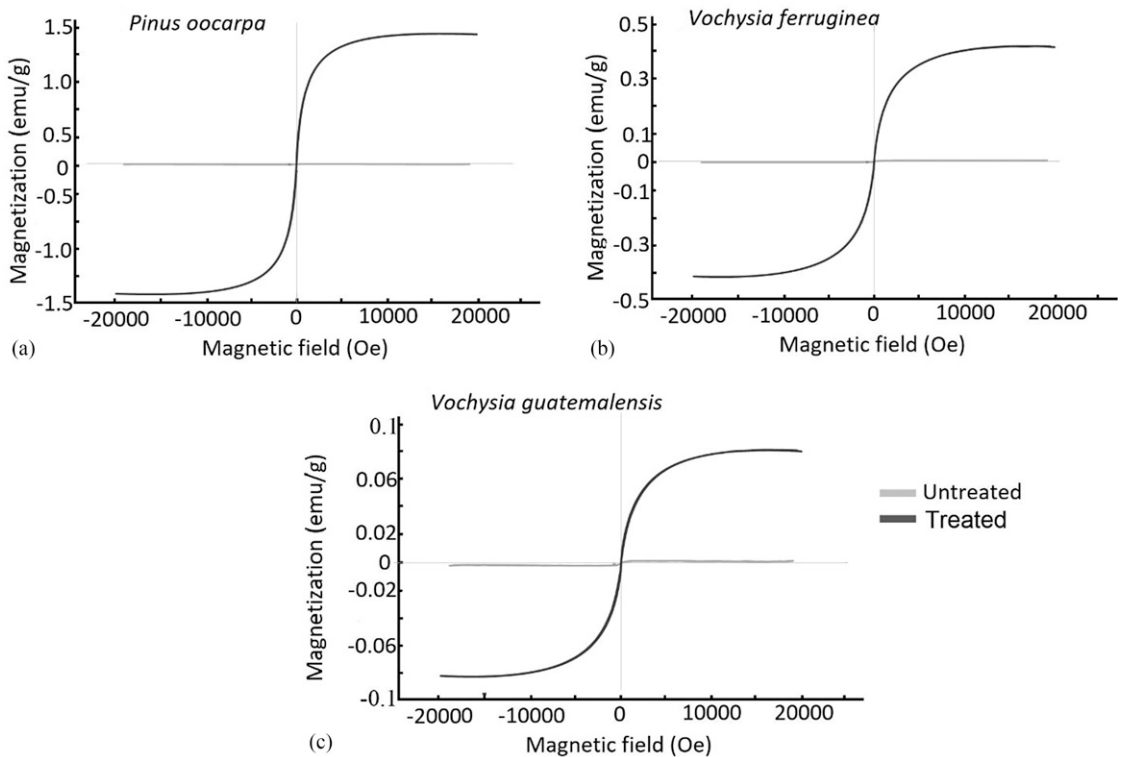


Figure 5. Magnetic hysteresis curves of three magnetic wood particleboards composite of tropical species (a-c) from fast growth plantations in Costa Rica.

in the dispersion of NPs along the samples (Lou et al 2019a), and since these measurements are made locally, ie, in different areas of the same sample, the values might change from one place to another, resulting in small differences in the magnetic values. This can be verified by the values that have been obtained in the three different samples of the same wood, where it can be seen that they have different amounts of NP.

In general, the values of H_c and M_s are low (Table 2), which indicates the magnetically soft

properties of the wood, compared with the results obtained previously by Moya et al (2022), which reported the highest values of M_s in *Vochysia ferruginea* and *Vochysia guatemalensis*, and similar values in *Pinus oocarpa*.

Regarding the process, Gan et al (2017a) indicated that alkaline immersion is more invasive of the structural components of wood than other magnetization methods. So, in the case of these species, the immersion time did not significantly alter the magnetic properties of the materials,

Table 1. The H_c , M_r , M_s , and the experimental percentage of three MWPC of tropical species from fast growth plantations in Costa Rica.

Species	H_c (Oe)	M_r (emu g ⁻¹)	M_s (emu g ⁻¹)	% experimental
<i>Pinus oocarpa</i>	11.94	0.02	1.39	9.04
<i>Vochysia ferruginea</i>	14.12	0.00	0.32	2.09
<i>Vochysia guatemalensis</i>	21.85	0.00	0.06	0.41

H_c , coercivity; M_r , retentivity; M_s , saturation magnetization; MWPC, magnetic wood particleboards composite.

Table 2. Physical properties of three MWPC of tropical species from fast growth plantations in Costa Rica.

Species	Treatment	Density (g cm ⁻³)	Thickness swelling (mm)	Moisture absorption (%)	Water absorption (%)
<i>Pinus oocarpa</i>	WPC	0.73 (1.62) ^{AB}	5.80 (6.19) ^B	4.90 (2.34) ^A	41.11 (4.42) ^A
	MWPC-layer	0.75 (2.20) ^A	6.84 (26.18) ^{AB}	4.84 (1.38) ^A	37.07 (1.68) ^B
	MWPC-100	0.74 (4.64) ^B	8.60 (22.88) ^A	4.25 (4.21) ^B	29.21 (16.06) ^C
<i>Vochysia ferruginea</i>	WPC	0.72 (2.18) ^B	8.78 (11.57) ^A	5.35 (1.98) ^A	45.60 (9.25) ^B
	MWPC-layer	0.74 (1.88) ^A	10.14 (36.11) ^A	4.33 (5.30) ^A	42.26 (7.71) ^B
	MWPC-100	0.73 (1.49) ^A	6.77 (19.79) ^A	4.39 (0.83) ^A	52.07 (8.57) ^A
<i>Vochysia guatemalensis</i>	WPC	0.73 (2.01) ^A	10.96 (36.18) ^A	5.31 (1.09) ^A	37.24 (13.03) ^{AB}
	MWPC-layer	0.74 (2.08) ^A	5.83 (22.09) ^B	4.83 (1.89) ^B	42.46 (7.56) ^B
	MWPC-100	0.73 (1.97) ^A	5.39 (24.12) ^B	4.39 (1.53) ^C	33.00 (16.91) ^A

Superscript letters mean statistical differences between treatments at 95% significance. And number in parentheses the coefficient of variation of the data.

MWPC, magnetic wood particleboards composite.

wood composites, although the immersion itself could affect the adhesion of the magnetic NPs in the samples.

Physical and Mechanical Properties

The results of the physical properties of the different particleboards (WPC, MWPC-100, and MWPC layers) are presented in Table 2. These results show that in *Pinus oocarpa* the density is higher in the MWPC layer and MWPC-100. The same situation was presented by the particleboards of *Vochysia ferruginea*, in which the density in MWPC-100 and the MWPC layers are higher. While in *Vochysia ferruginea*, there were no differences in density (Table 2). In the case of swelling in thickness, *Pinus oocarpa* particleboards with magnetic particles presented greater swelling. On the contrary, the *Vochysia guatemalensis* boards decreased the swelling values with magnetization and, in the case of *Vochysia ferruginea*, there were no differences (Table 2).

In the case of moisture absorption, this value decreased statistically with the magnetization of the *Pinus oocarpa* particleboard material from MWPC-100. This same effect is observed in *Vochysia guatemalensis*, where the lowest value of moisture absorption was presented in the MWPC-100 and the highest in MPC. For the *Vochysia ferruginea* particleboards, there were no differences between the different treatments (Table 2). For the capability of water absorption, in the case of the *Pinus oocarpa*, MWPC shows a

higher absorption, while MWPC-100 shows a lower absorption. In *Vochysia ferruginea*, the MWPC-100 treatment shows higher values. Finally, in *Vochysia guatemalensis*, the highest percentage of water absorption occurs in the MWPC layer (Table 2).

The slight differences between the densities of the WPC in the three types of treatments and, in all the species studied, may be related to the fact that the pressing process was very similar (temperature, time, and pressure) for all the particleboards under the same conditions. On the other hand, the swelling of the thickness did not present a clear trend in the three species, but a high variation in the results was observed. As for the MC, it is observed that there was a decreasing trend in the values with respect to the control, which is due to the chemical synthesis of the Fe₃O₄ NPs in the material since the amorphous fractions in the cellulose decreases the access to moisture and water absorption (Mashkour and Ranjbar 2018). The same situation occurs in the water absorption, especially in *Pinus oocarpa* where in MWPC-layer and MWPC-100, a decrease is observed compared with WPC (Table 2), meaning that in this species the synthesis of Fe₃O₄ was carried out correctly. On the other hand, the increase of the water absorption in MWPC-layer and MWPC-100 in *Vochysia ferruginea* and the *Vochysia guatemalensis* with respect to WPC (Table 2) is attributed to the fact that during the magnetic treatment, the acidic condition of the ferric and ferrous chloride solution, and the subsequent basic

Table 3. Mechanical properties of three MWPC of tropical species from fast growth plantations in Costa Rica.

Species	Treatment	Internal bond (MPa)	Hardness (N)
<i>Pinus oocarpa</i>	WPC	0.70 (21.61) ^A	8.60 (6.97) ^B
	MWPC-layer	0.65 (38.53) ^A	11.37 (3.48) ^A
	MWPC-100	0.57 (47.65) ^A	6.99 (11.08) ^C
<i>Vochysia ferruginea</i>	WPC	0.64 (26.08) ^A	9.70 (11.08) ^B
	MWPC-layer	0.67 (24.79) ^A	10.82 (11.97) ^{AB}
	MWPC-100	0.17 (49.90) ^B	11.30 (11.35) ^A
<i>Vochysia guatemalensis</i>	WPC	0.50 (24.93) ^A	12.85 (21.74) ^B
	MWPC-layer	0.39 (53.71) ^{AB}	15.96 (20.24) ^{AB}
	MWPC-100	0.26 (30.75) ^B	17.51 (16.06) ^B

Superscript letters mean statistical differences between treatments at 95% significance. And number in parentheses the coefficient of variation of the data.

MWPC, magnetic wood particleboards composite.

condition of the aqueous ammonia solution lead to a partial decomposition and collapse of the wood components (Dong et al 2016), which damages the wood and contributes to water absorption.

Regarding the mechanical properties, it was observed that the internal bond decreased in the MWPC (Table 3). In *Pinus oocarpa*, there was no statistical difference in the property of internal bond, while in *Vochysia ferruginea* and *Vochysia guatemalensis*, the value decreased significantly in MWPC-100, but in both the species the MWPC layer treatment did not present differences with WPC (Table 3). Regarding the hardness in *Pinus oocarpa*, it increased significantly in the MWPC layer but decreased in MWPC-100. In *Vochysia ferruginea* and *Vochysia guatemalensis*, the hardness value increased in MWPC-100 and the MWPC layer (Table 3).

When comparing the results of internal bonds with other works, in *Pinus oocarpa*, the values are between the range obtained by Santos et al (2021), where it presents internal bond values between 0.42 and 0.66 MPa. In the case of *Vochysias*, the values obtained are compared with those obtained by Rigg-Aguilar et al (2019), which reported internal bond values between 0.14 and 0.589 MPa. On the other hand, the decrease in this property with magnetism can be attributed to the collapse of the wood components with the treatment (Lou et al 2019a). A collapse in the bonds of cellulose and lignin results in there being no effective interaction between the hydroxyl groups of the cellulose and the urea-formaldehyde adhesive (Sheng Han et al 2006) used in the elaboration of the WPC (Figure 6). Regarding the hardness, it was possible to observe that this property improves slightly with magnetism, especially

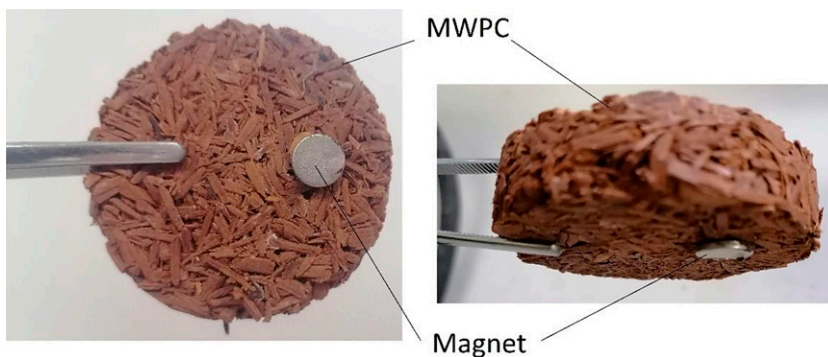


Figure 6. A magnetized sample of magnetic wood particleboards composite (MWPC) for *Pinus oocarpa*, attracted by a magnet.

in the Vochyseas (Table 3). This can be attributed to the Fe_3O_4 NPs, as they create a higher resistance on the surface of the MWPC (Martins et al 2021), which makes the material more resistant to mechanical stress on the surface.

CONCLUSION

The use of wood composites with fiber magnetized with Fe_3O_4 NPs and synthesized in situ by means of an in-situ impregnation of Fe^{3+} and Fe^{2+} and immersed in ammonia in three tropical species (*Pinus oocarpa*, *Vochysia ferruginea*, and *Vochysia guatemalensis*) presented low values of Hc, Mr, and Ms compared with solid wood of this species or other species, which is attributed to the low permeability and penetration of solutions in the species. The least precipitation occurred in *Pinus oocarpa*, but it presented better magnetic properties and, on the contrary, the species with less magnetic properties were *Vochysia guatemalensis* and *Vochysia ferruginea*. Despite the little effect on MWPC, there was evidence of changes in the chemical components of the wood, a decrease in density, an increase in swelling and moisture absorption, and a few changes in the mechanical properties of the wood because immersion in ammonia produces changes in the chemical components of wood. In general, the in-situ precipitation by immersion limits the synthesis of the NPs within the wood, to this added the size of the wood fiber, which makes the impregnated surface smaller, therefore the magnetic data were reduced.

ACKNOWLEDGMENTS

The authors thank to Vicerrectoría de Investigación y extensión of the Instituto Tecnológico de Costa Rica for the financial support to develop the project.

REFERENCES

- ASTM (1985) Standard test method for anti-swelling effectiveness of water-repellent formulations and differential swelling of untreated wood when exposed to liquid water environments. Annu B ASTM 4:702-706. doi: 10.1520/D4446-08R12.when.
- ASTM (1999) Standard guide for moisture conditioning of wood and wood-based materials. Current i:1-8. doi: 10.1520/D4933-99R10.2.
- ASTM (2013) Standard test method for ash in wood. Annu B ASTM Stand 410:1-2.
- ASTM (2021) Test methods for determination of trace elements in coal, coke, & combustion residues from coal utilization processes by inductively coupled plasma atomic emission, inductively coupled plasma mass, & graphite furnace atomic absorption spec. Annu B ASTM Stand 5:406-410.
- Bolton AJ, Humphrey PE (1994) The permeability of wood-based composite materials: Part 1. A review of the literature and some unpublished work. Holzforschung 48: 95-100. doi: 10.1515/HFSG.1994.48.S1.95/HTML.
- Cave I, Walker J (1994) Stiffness of wood in fast-grown plantation softwoods: The influence of microfibril angle. Forest Prod J 44:43-48.
- Dong Y, Yan Y, Zhang S, Li S, Wang J (2015) Flammability and physical-mechanical properties assessment of wood treated with furfuryl alcohol and nano- SiO_2 . Eur J Wood Wood Prod 73:457-464. doi: 10.1007/s00107-015-0896-y.
- Dong Y, Yan Y, Zhang Y, Li J (2016) Combined treatment for conversion of fast-growing poplar wood to magnetic wood with high dimensional stability. Springer 50:503-517. doi: 10.1007/s00226-015-0789-6.
- Gaitán-Alvarez J, Berrocal A, Mantanis GI, Moya R, Araya F (2020a) Acetylation of tropical hardwood species from forest plantations in Costa Rica: An FTIR spectroscopic analysis. J Wood Sci 66:1-49. doi: 10.1186/s10086-020-01898-9.
- Gaitán-Alvarez J, Moya R, Berrocal A, Araya F (2020b) In-situ mineralization of calcium carbonate of tropical hardwood species from fast-grown plantations in Costa Rica. Carbonates Evaporites 29:09184-9144.
- Gaitán-Alvarez J, Moya R, Mantanis GI, Berrocal A (2021) Furfurylation of tropical wood species with and without silver nanoparticles: Part I: Analysis with confocal laser scanning microscopy and FTIR spectroscopy. Wood Mater Sci Eng 17:410-419. doi: 10.1080/17480272.2021.1886166.
- Gan W, Gao L, Liu Y, Zhang Y, Li J (2016) The magnetic, mechanical, thermal properties and UV resistance of $\text{CoFe}_2\text{O}_4/\text{SiO}_2$ -coated film on wood. J Wood Chem Technol 36:94-104. doi: 10.1080/02773813.2015.1074247.
- Gan W, Gao L, Xiao S, Zhang S, Zhan W, Li J (2017a) Transparent magnetic wood composites based on immobilizing Fe_3O_4 nanoparticles into a delignified wood template. J Mater Sci 52:3321-3329. doi: 10.1007/s10853-016-0619-8.
- Gan W, Liu Y, Gao L, Zhan X, Li J (2017b) Magnetic property, thermal stability, UV-resistance, and moisture absorption behavior of magnetic wood composites. Wiley Online Libr 38:1646-1654. doi: 10.1002/pc.23733.
- Gao HL, Wu GY, Guan HT, Zhang GL (2012) In situ preparation and magnetic properties of Fe_3O_4 /wood composite. Mater Technol 27:101-103. doi: 10.1179/175355511X13240279339806.
- Gao X, Dong Y, Wang K, Chen Z, Yan Y, Li J, Zhang S (2017) Improving dimensional and thermal stability of

- poplar wood via aluminum-based sol-gel and furfurylation combination treatment. *BioResources* 12 2:3277-3288. doi: 10.15376/biores.12.2.3277-3288.
- Garskaite E, Stoll SL, Forsberg F, Lycksam H, Stankeviciute Z, Kareiva A, Quintana A, Jensen CJ, Liu K, Sandberg D (2021) The accessibility of the cell wall in scots pine (*Pinus sylvestris* L.) sapwood to colloidal Fe₃O₄ nanoparticles. *ACS Omega* 6:21719-21729. doi: 10.1021/acsoomega.1c03204.
- Kojima M, Yamamoto H, Marsoem SN, Okuyama T, Yoshida M, Nakai T, Yamashita S, Saegusa K, Matsune K, Nakamura K, Inoue Y, Arizono T (2009) Effects of the lateral growth rate on wood quality of *Gmelina arborea* from 3.5-, 7- and 12-year-old plantations. *Ann Sci* 66: 507. doi: 10.1051/forest/2009031.
- Lin C-C, Ho J-M (2014) Structural analysis and catalytic activity of Fe₃O₄ nanoparticles prepared by a facile co-precipitation method in a rotating packed bed. *Ceram Int* 40:10275-10282. doi: 10.1016/j.ceramint.2014.02.119.
- Liu J, Che R, Chen H, Zhang F, Xia F, Wu Q, Wang M (2012) Microwave absorption enhancement of multifunctional composite microspheres with spinel Fe₃O₄ cores and anatase TiO₂ shells. *Small* 8:1214-1221. doi: 10.1002/sml.201102245.
- Lou Z, Han H, Zhou M, Han M, Cai J, Huang C, Sun Z (2018a) Synthesis of magnetic wood with excellent and tunable electromagnetic wave-absorbing properties by a facile vacuum/pressure impregnation method. *ACS Sustain Chem Eng* 6:1000-1008. doi: 10.1021/acssuschemeng.7b03332.
- Lou Z, Wang W, Yuan C, Zhang Y, Li Y, Yang L (2019a) Fabrication of Fe/C composites as effective electromagnetic wave absorber by carbonization of pre-magnetized natural wood fibers. *J Bioresour Bioprod* 4:43-50. doi: 10.21967/jbb.v4i1.185.
- Lou Z, Yuan C, Zhang Y, Li Y, Cai J, Yang L, Zou J (2019b) Synthesis of porous carbon matrix with inlaid Fe₃C/Fe₃O₄ micro-particles as an effective electromagnetic wave absorber from natural wood shavings. *J Alloys Compd* 775:800-809. doi: 10.1016/j.jallcom.2018.10.213.
- Lou Z, Zhang Y, Zhou M, Han M, Cai J, Yang L, Li Y (2018b) Synthesis of magnetic wood fiber board and corresponding multi-layer magnetic composite board, with electromagnetic wave absorbing properties. *Nano-materials* 8(6):441. doi: 10.3390/nano8060441.
- Lv H, Yang Z, Wang PL, Ji PL, Song J, Zheng L, Xu ZJ (2018) A voltage-boosting strategy enabling a low-frequency, flexible electromagnetic wave absorption device. *Adv Mater* 30:1706343. doi: 10.1002/adma.201706343.
- Martins RSF, Gonçalves FG, Segundinho PGdA, Lelis PG, Paes JB, Lopez YM, Oliveira RG (2021) Investigation of agro-industrial lignocellulosic wastes in fabrication of particleboard for construction use. *J Build Eng* 43:102903. doi: 10.1016/j.job.2021.102903.
- Mashkour M, Ranjbar Y (2018) Superparamagnetic Fe₃O₄ wood flour/polypropylene nanocomposites: Physical and mechanical properties. *Ind Crops Prod* 111:47-54. doi: 10.1016/j.indcrop.2017.09.068.
- Moya R, Gaitán-Alvarez J, Berrocal A, Araya F (2020) Effect of CaCO₃ in the wood properties of tropical hardwood species from fast-grown plantation in Costa Rica. *BioResources* 15:4802-4822.
- Moya R, Gaitán-Alvarez J, Berrocal A, Merazzo KJ (2022) *In Situ Synthesis* of Fe₃O₄ nanoparticles and wood composite properties of three tropical species. *Materials (Basel)* 15:3394. doi: 10.3390/ma15093394.
- Moya-Roque R, Camacho D, Soto-Fallas R, Mata-Segreda J (2014) Internal bond strength of particle boards manufactured from a mixture of *Gmelina arborea*, *Tectona grandis* and *Cupressus lusitanica* with the fruit of *Elaeis guineensis*, leaves of *Ananas comosus* and tetra pak packages. *Rev For Mesoam Kurú* 12:36. doi: 10.18845/rfink.v12i28.2098.
- Oka H, Hamano H, Chiba S (2004a) Experimental study on actuation functions of coating-type magnetic wood. *J Magn Magn Mater* 272:E1693-E1694.
- Oka H, Hojo A, Osada H, Namizaki Y, Taniuchi H (2004b) Manufacturing methods and magnetic characteristics of magnetic wood. *J Magn Magn Mater* 272:2332-2334.
- Oka H, Kataoka Y, Osada H, Aruga Y, Izumida F (2007) Experimental study on electromagnetic wave absorbing control of coating-type magnetic wood using a grooving process. *J Magn Magn Mater* 310:e1028-e1029. doi: 10.1016/j.jmmm.2006.11.073.
- Oka H, Narita K, Osada H, Seki K (2002) Experimental results on indoor electromagnetic wave absorber using magnetic wood. *J Appl Physics* 91:7008-7010. doi: 10.1063/1.1448796.
- Oka H, Tanaka K, Osada H, Kubota K, Dawson FP (2009) Study of electromagnetic wave absorption characteristics and component parameters of laminated-type magnetic wood with stainless steel and ferrite powder for use as building materials. *J Appl Phys* 105:07E701. doi: 10.1063/1.3056403.
- Oka H, Terui M, Osada H, Sekino N, Namizaki Y, Oka H, Dawson FP (2012) Electromagnetic wave absorption characteristics adjustment method of recycled powder-type magnetic wood for use as a building material. *IEEE Trans Magn* 48:3498-3500. doi: 10.1109/TMAG.2012.2196026.
- Rahayu I, Prihatini E, Ismail R, Darmawan W, Karlinasari L, Laksono GD (2022) Fast-growing magnetic wood synthesis by an in-situ method. *Polymers (Basel)* 14: 2137. doi: 10.3390/polym14112137.
- Rao X, Liu Y, Fu Y, Liu Y, Yu H (2016) Formation and properties of polyelectrolytes/TiO₂ composite coating on wood surfaces through layer-by-layer assembly method. *Holzforchung* 70:361-367. doi: 10.1515/hf-2015-0047.
- Rennekar S, Zhou Y (2009) Nanoscale coatings on wood: Polyelectrolyte adsorption and layer-by-layer assembled film formation. *ACS Appl Mater Interfaces* 1:559-566. doi: 10.1021/am800119q.

- Rigg-Aguilar P, Moya R, Vega-Baudrit J, Navarro-Mora A, Gaitán-Alvarez J (2019) European pallets fabricated with composite wood blocks from tropical species reinforced with nanocrystalline cellulose: Effects on the properties of blocks and static flexure of the pallet. *BioResources* 14(2):3651-3667. doi: 10.15376/biores.14.2.3651-3667.
- Santos J, Pereira J, Ferreira N, Paiva N, Ferra J, Magalhaes FD, Carvalho LH (2021) Valorisation of non-timber by-products from maritime pine (*Pinus pinaster*, Ait) for particleboard production. *Ind Crops Prod* 168:113581. doi: 10.1016/j.indcrop.2021.113581.
- Sheng Han Y, Hadiko G, Fuji M, Takahashi M (2006) Crystallization and transformation of vaterite at controlled pH. *J Cryst Growth* 289:269-274. doi: 10.1016/j.jcrysgro.2005.11.011.
- Tang T, Fu Y (2020) Formation of chitosan/sodium phytate/nano-Fe₃O₄ magnetic coatings on wood surfaces via layer-by-layer self-assembly. *Coatings* 10:51. doi: 10.3390/coatings10010051.
- Tenorio C, Moya R, Salas C, Berrocal A (2016) Evaluation of wood properties from six native species of forest plantations in Costa Rica. *Bosque (Valdivia)* 37:71-84. doi: 10.4067/S0717-92002016000100008.
- Thomas RJ (1976) Anatomical features affecting liquid penetrability in three hardwood species. *Wood Fiber Sci* 4:256-263.
- Trey S, Olsson RT, Ström V, Berglund L, Johansson M (2014) Controlled deposition of magnetic particles within the 3-D template of wood: Making use of the natural hierarchical structure of wood. *RSC Adv* 4:35678-35685. doi: 10.1039/c4ra04715j.
- Wang H, Yao Q, Wang C, Ma Z, Sun Q, Fan B, Chen Y (2017) Hydrothermal synthesis of nanooctahedra mfe2o4 onto the wood surface with soft magnetism, fire resistance and electromagnetic wave absorption. *Nanomaterials (Basel)* 7:118. doi: 10.3390/nano7060118.
- Wang L, Li N, Zhao T, Li B, Ji Y (2019) Magnetic properties of FeNi₃ nanoparticle modified *Pinus radiata* wood nanocomposites. *Polymers (Basel)* 11:421. doi: 10.3390/polym11030421.
- Yang L, Lou Z, Han X, Liu J, Wang Z, Zhang Y, Li Y (2020) Fabrication of a novel magnetic reconstituted bamboo with mildew resistance properties. *Mater Today Commun* 23:101086. doi: 10.1016/j.mtcomm.2020.101086.
- Zheng J, Lv H, Lin X, Ji G, Li X, Du Y (2014) Enhanced microwave electromagnetic properties of Fe₃O₄/graphene nanosheet composites. *J Alloys Compd* 589:174-181. doi: 10.1016/j.jallcom.2013.11.114.